Synthesis and Structure of As-Prepared ITQ-4, A Large Pore Pure Silica Zeolite: The Role and Location of Fluoride Anions and Organic Cations

P. A. Barrett,[†] M. A. Camblor,*[,†] A. Corma,[†] R. H. Jones,[‡] and L. A. Villaescusa[†]

Instituto de Tecnología Química, CSIC-UPV, Universidad Politécnica de Valencia, Avda. Los Naranjos s/n, 46071 Valencia, Spain, and Department of Chemistry, University of Keele, Keele, Staffordshire, ST5 5BG U.K.

Received: January 9, 1998; In Final Form: March 13, 1998

Pure silica ITQ-4, a zeolitic material with large one-dimensional 12MR channels and an unexpectedly large microporous void volume, can be synthesized in the presence of fluoride ions and *N*-benzylquinuclidinium cations within a wide range of synthesis pH. Substitution of the tertiary carbon of the quinuclidine moiety by a N atom still renders the organic cation as a suitable structure-directing agent for this material. The role of F^- anions and the influence of the pH of the synthesis on both the phase selectivity of the crystallization and the presence of connectivity defects in the final material are discussed. In the presence of F^-, defect formation is observed to be pH-dependent, and there appears to be a threshold pH for the generation of a constant defect concentration. A plausible explanation for this observation based upon the ionization state of the condensing species is also presented. The structure of as-made ITQ-4 has been obtained and refined from high-resolution powder XRD data, and the organic and fluoride ions have been located. The sinuosity of the channel of ITQ-4 is found to coincide with the bent geometry observed for the structure-directing agent, while the fluoride ions are found to reside within a small $[4^3 5^2 6]$ cage located around the periphery of the central pore space.

Introduction

Silica-based microporous materials can be synthesized through two different hydrothermal (or solvothermal) synthetic routes. One makes use of the hydroxide anion as a mineralizer and usually takes place at high pH,[1] while in the other the F^- anion is the mineralizer and the synthesis is carried out at near neutral (or slightly alkaline) pH.[2] The use of one or another mineralizer is not trivial, because the nature and properties of the final material can heavily depend on this choice. In general, high-silica zeolites synthesized at high pH have a significant concentration of connectivity defects. Although this is primarily related to the need to counterbalance the positive charge of the organic additives that end up occluded within the zeolitic voids, generally a much higher concentration of such defects is found.[3] On the contrary, materials prepared in F^- aqueous media usually show a small concentration of such defects, which in turn can affect the polar properties of the microporous surface of the material and can ultimately influence its catalytic properties.[4] Additionally, F^- ions can determine the phase selectivity during the crystallization and in this respect are sometimes claimed to be a structure-directing agent and even a "template" in the synthesis of zeolites.[5] In any case what appears to be certain is that F^- ions seem especially suited to allow the synthesis of very high silica zeolites or even pure silica polymorphs.

The F^- synthesis route, first introduced in the late 1970s, has been particularly used for the preparation of high-silica zeolites. However, there has been little by way of discussion on the key factors that govern the phase selectivity during the crystallization and on the reasons for the final properties of the materials, characterized by their low concentration of connectivity defects. For most of the zeolites prepared by this route the location of F^- in the zeolite structure is still unknown and its role during the crystallization is not well understood. We have very recently started a project on the synthesis of zeolites by the fluoride route that has already extended the kind of materials prepared and importantly has been able to demonstrate the feasibility of producing very low framework density materials that seemed to be difficult to synthesize in conventional OH^- media as pure silica polymorphs. Thus, defect-free pure silica phases with framework densities of 15.6 (Beta, BEA),[6] 16.3 (ITQ-3, ITE),[7] and 17.0 (ITQ-4, IFR)[8] Si per 1000 $Å^3$ have been recently synthesized in fluoride media. In an attempt to better understand the role of F^- during the crystallization and its influence on the final materials, we present here the synthesis of pure silica ITQ-4 (IFR) and discuss the mechanism of crystallization relating to the formation of connectivity defects. We also present the crystalline structure of the as-made material, where the locations of both the organic structure-directing agent and the fluoride anion have been determined.

Experimental Section

Synthesis. The syntheses of ITQ-4 were carried out hydrothermally in the absence of alkali cations, using *N*-benzylquinuclidinium (**I**) or *N*-benzyl-1,4-diazabiciclo[2.2.2]octane (**II**) as organic structure-directing agents (SDAs). These were obtained in high yields by reaction of the corresponding amine (quinuclidine or diazabicyclooctane) as a free base or in its hydrochloride form (in this case an inorganic base such as $K_2CO_3 \cdot 1.5H_2O$ is also added to liberate the free amine) with an excess of benzyl chloride in chloroform at room temperature. After separation and washing with ethyl acetate, the chloride salt was anion exchanged with a Dowex resin to obtain the hydroxide form, which was then titrated to determine the degree

* Corresponding author: Dr. M. A. Camblor, macamblo@itq.upv.es. Fax: 34-6-3877809.
[†] Universidad Politécnica de Valencia.
[‡] University of Keele.

S1089-5647(98)00735-4 CCC: $15.00
Published on Web 05/02/1998

TABLE 1: Summary of Synthesis Conditions and Results

composition[a] per SiO_2	temperature/ °C	time/ days	final pH	solid
$0.5HF:0.5R_IOH:15H_2O$	150	9	8.1	ITQ-4
		13	8.2	ITQ-4
$0.55HF:0.5R_IOH:15H_2O$	175	27	7.0	ITQ-4
$0.5NH_4F:0.5R_IOH:14H_2O$	150	13	10.0	ITQ-4
$0.5R_IOH:15H_2O$	150	13	11.9	La[b]
$0.5HF:0.5R_IOH:6.8H_2O$	135	3.6	7.7	ITQ-4
$0.5HF:0.5R_IOH:4.4H_2O$	175	6	7.7	ITQ-4
$0.5NH_4F:0.75R_IOH:15H_2O$	150	12	11.2	ITQ-4
$0.5HF:0.5R_{II}OH:5.2H_2O$	175	3	8.3	ITQ-4

[a] R_IOH and $R_{II}OH$ represent the *N*-benzylquinuclidinium (SDA **I**) hydroxide and the *N*-benzyl-1,4-diazabiciclo[2.2.2]octane (SDA **II**) monohydroxide, respectively. [b] Unknown, probably layered phase.

of exchange (typically above 90%). In the chemical composition of the synthesis gels (listed in Table 1) the organic hydroxide content is based on the OH^- content. For the synthesis of ITQ-4, tetraethyl orthosilicate (TEOS) was hydrolyzed at room temperature in a titrated solution of the hydroxide form of SDA **I** or **II**, and the mixture was stirred for several hours allowing for the complete evaporation of the ethanol produced (plus some water). The chemical compositions listed in Table 1 account for the final composition; that is, evaporation of water has been taken into account. After this process no ethanol could be detected by ^1H NMR, suggesting that there is no azeotrope in these conditions, contrary to the well-known behavior of pure ethanol/water mixtures. Then, the required amount of HF (48% aqueous solution, Merck) was added, and the thick gel obtained was thoroughly homogenized by hand. Finally, it was charged into 60 mL Teflon lined stainless steel autoclaves, which were rotated at 60 rpm at the crystallization temperature (423 or 448 K). The solids were then recovered by filtration, washed with distillate water, and dried at 373 K. When required, the solids were calcined at 580 °C in air to remove the organic structure-directing agent and the fluorine occluded during the synthesis.

Characterization. Phase purity and crystallinity were determined by conventional powder X-ray diffraction (XRD) using a Philips X'Pert diffractometer (Cu Kα radiation provided by a graphite monochromator) equipped with a variable divergence slit and working in the fixed irradiated area mode. C, H, and N contents were determined with a Carlo Erba 1106 elemental organic analyzer. The fluoride content was determined using an ion-selective electrode connected to a Mettler Toledo 355 ion analyzer after dissolution of the as-made solids by a standard procedure.[9] MAS NMR spectra of the solids were recorded on a Varian VXR 400SWB spectrometer. The ^{29}Si MAS NMR spectra were recorded with a spinning rate of 5.5 kHz at a ^{29}Si frequency of 79.459 MHz with a 55.4° pulse length of 4.0 μs and a recycle delay of 60 s. The $^1H \rightarrow ^{13}C$ CPMAS NMR spectra were acquired with a spinning rate of 5 kHz at a ^{13}C frequency of 100.579 MHz with a 90° pulse length of 7.5 μs, a contact time of 5000 μs, and a recycle delay of 2 s. Both ^{29}Si and ^{13}C chemical shifts are reported relative to TMS. N_2 and Ar adsorption/desorption experiments were undertaken isothermally at 77 and 87.3 K, respectively, using an automatic ASAP 2000 Micromeritics apparatus. The infrared spectrum in the region of framework vibrations (300−1900 cm^{-1}) was recorded using a Nicolet 710 FTIR spectrometer and the KBr pellet technique for sample preparation. Finally, crystal size and morphology were monitored by scanning electron microscopy (SEM) using a JEOL JSM-6300 microscope.

Synchrotron Data Collection. High-resolution powder X-ray diffraction data were collected on station 2.3 of the Daresbury Synchrotron Radiation Source. The as-prepared ITQ-4 sample was mounted in a Perspex sample holder at 298 K and rotated to obtain better powder averaging. The data were collected in flat plate geometry[10] using the data collection parameters summarized in Table 4. The wavelength prior to measurement was calibrated using a Si NBS standard.

TABLE 2: Chemical Composition of ITQ-4 Samples

SDA	final pH	mol/100g of as-made sample N	C	H	F	C/N	mol/uc R[a]	F
I	8.0	0.0854	1.2020	1.7283	0.090	14.1	2.13	2.20
I	10.0	0.0842	1.1469	1.7098	0.077	13.6	1.99	1.81
I	10.4	0.0887	1.2319	1.9251	0.046	13.9	2.16	1.13
I	11.2	0.0892	1.2225	1.8640	0.050	13.7	2.14	1.20
II	8.4	0.1327	0.8195	1.3160		6.2	1.6	
II	9.6	0.2073	1.1285	1.7620		5.4	2.5	

[a] R represents the structure directing agents **I** or **II**.

TABLE 3: Comparison of the Intrazeolitic Void Spaces of the Pure Silica Polymorphs with the Lowest Framework Densities

material	code	void volume ($cm^3\ g^{-1}$)	FD (T/1000 $Å^3$)[a]	channel system	ref
ITQ-4	IFR	0.217	17.0	1D, 12MR	this work
ITQ-1	MWW	0.17	16.5	2D, 10MR + 12MR cages	33, 34
ITQ-3	ITE	0.23	16.3	2D, 8MR	7
Beta	BEA*	0.22	15.6	3D, 12MR	6

[a] Determined from the unit cell parameters of the pure silica polymorph and the reported structure.

TABLE 4: Data Collection and Crystallographic Data for As-Prepared ITQ-4

wavelength	1.39996 Å
temperature	298 K
2θ range	6−80°
step size	0.01°
count time	$2\theta = 6-33°$ 2s/p $2\theta = 33-80°$ 4s/p
number of data points	7699
number of reflections	840
number of profile parameters	11
number of structural parameters	70
number of constraints	29
unit cell *a*	18.49612(10) Å
b	13.44060(5) Å
c	7.71112(5) Å
β	101.5768(5)°
space group	*I*2/*m*
residuals R_p	7.99
R_{wp}	10.44
R_b	10.06
χ^2	2.69

Results and Discussion

Synthesis. A summary of synthesis conditions and results is given in Table 1. In the synthesis conditions reported here we were able to synthesize highly crystalline ITQ-4[11] as a new pure silica polymorph[12] using two closely related organic additives: *N*-benzylquinuclidinium (SDA **I**) and *N*-benzyl-1,4-diazabiciclo[2.2.2]octane (SDA **II**). This is not surprising because **II** is formally obtained by substituting the tertiary carbon of the quinuclidine moiety of **I** by a nitrogen atom, and thus the basic geometry, shape, and size of the original SDA is preserved. However, the stability of these two organic additives in the synthesis medium appears to be different (see below).

It is interesting to note that, albeit ITQ-4 seems to be isomorphous to zeolites SSZ-42[13] and MCM-58,[14] which can

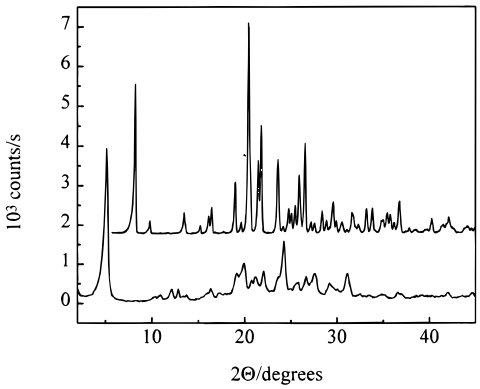

Figure 1. X-ray diffraction patterns of as-made pure silica ITQ-4 (top) and the phase obtained in the absence of F^- (bottom, denoted as La in Table 1).

be synthesized using the same structure-directing agent (**I**), the range of chemical compositions directly attainable by synthesis differ largely for ITQ-4, which has been synthesized in the Si/Al range 20−∞.[15] On the other hand MCM-58 (whose Si/Al ratio is claimed in the 5−500, 5−200, or 10−100 ranges in different parts of the patent) appears to be difficult to synthesize as a pure phase outside the range Si/Al = 12−33, according to the reported syntheses (with mordenite and quartz cocrystallizing with MCM-58 when the Si/Al ratio in the gel is decreased below 15 or increased above 35, respectively).[14] On the other hand, the synthesis of SSZ-42 also seems to require the presence of a trivalent element in the nutrient gel (preferred Si/T(III) = 7.5−50), with the added constraint that at least 50% of it must be boron.[13] In view of the close similarity of the XRD patterns of all three materials and the basically coincident framework topologies proposed for ITQ-4[8] and SSZ-42,[20] all three materials appear to be isomorphous. Thus, the differences in the attainable range of chemical composition must be directly related to the synthesis conditions employed in each case. These are very similar for SSZ-42 and MCM-58, which are synthesized from mixtures containing alkali cations at a high pH. The main differences are that for SSZ-42 boron is always used with small amounts of Na^+ and the crystallization is carried at 150 °C in static conditions, while for MCM-58 large amounts of K^+ are added and the synthesis is performed at 170 °C in a stirred autoclave. For ITQ-4, the use of F^- anions in a mixture free of alkali cations at near neutral pH therefore marks a significant deviation from the more conventional conditions employed for the other materials and provides a likely cause for the different range of chemical compositions attainable from the two synthesis methods. When HF is not added in a synthesis of pure silica ITQ-4 (pH = 11.5−12), a phase of unknown structure and low thermal stability (possibly a layered material) crystallizes instead (Table 1 and Figure 1).

Since the pioneering work by Flanigen and Patton,[16] the feasibility of synthesizing pure silica phases isomorphous to Al-containing zeolites[5,6] through the use of F^- as a mineralizer at near neutral pH has been demonstrated. In an attempt to clarify whether the important parameter in the synthesis of pure silica ITQ-4 is the pH or the presence of F^-, we performed several experiments in which the F^- anion is added as HF or NH_4F or mixtures of both (so as to preserve the F^- concentration while varying the pH in the range 7−10), and all of them yielded pure ITQ-4. As the pH was not as high in these experiments as in the case when no F^- was added, we designed another experiment in which extra *N*-benzylquinuclidinium hydroxide was added, and again ITQ-4 was the only product obtained (final pH = 11.2). These results demonstrate that the key parameter for the synthesis of ITQ-4 is the presence of F^- anions, with a wide tolerance existing toward changes in pH.

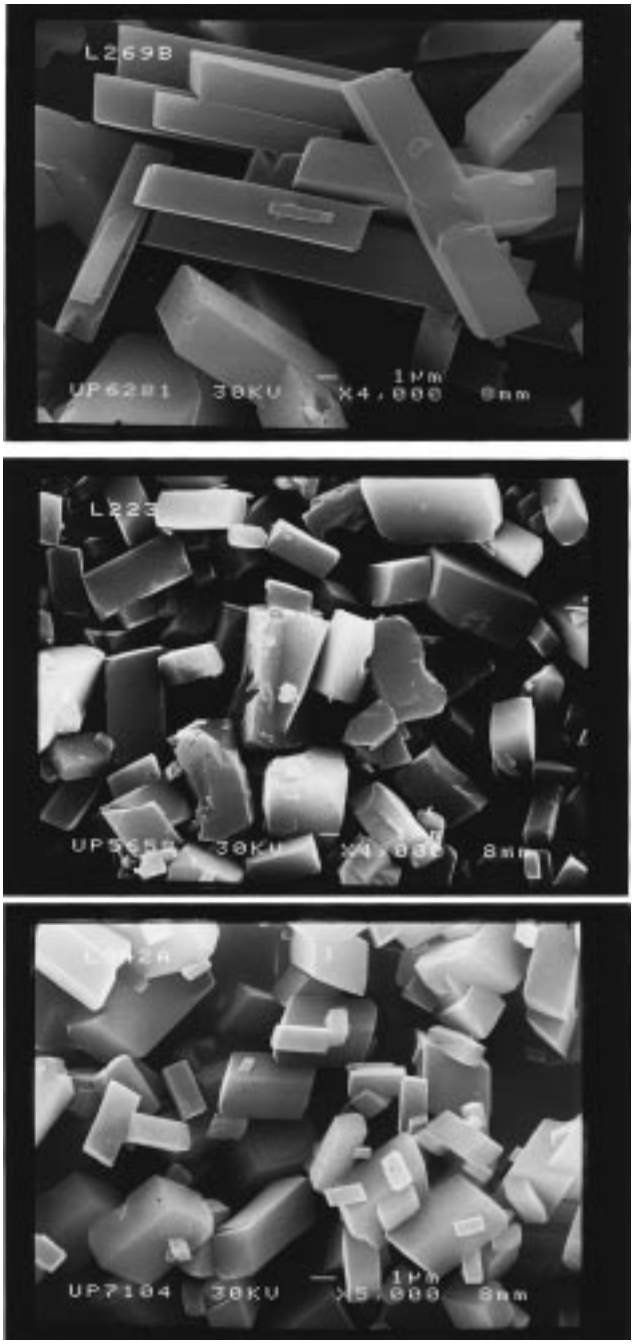

Figure 2. SEM of as-prepared ITQ-4 samples showing the elongated shape of the crystallites and the typical change in the aspect ratio as the synthesis pH increases (pH = 8, 10.4, and 11.2 from top to bottom).

Characterization. Pure silica ITQ-4 typically displays an elongated crystallite morphology of several micrometers in length, as shown in Figure 2. However, the aspect ratio of the crystals depends on the pH conditions of the synthesis. As seen in Figure 2, at near to neutral pH the crystals are more elongated (aspect ratio, defined as long edge to short edge ratio, typically exceeding 5) than the ones obtained in more alkaline conditions (aspect ratio typically below 2.5).

In addition to its characteristic XRD pattern (Figure 1, top), ITQ-4 can be distinguished from other zeolites by means of its well-resolved infrared spectrum, which shows very sharp bands in the 500−750 cm^{-1} region, which constitute fingerprint features for this material (Figure 3).

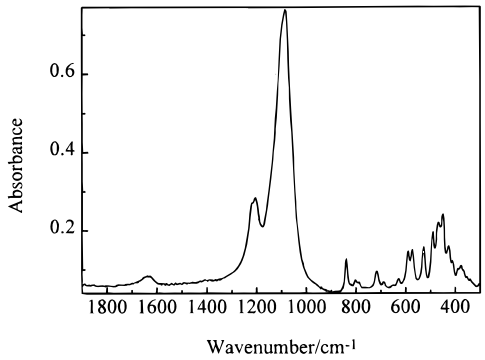

Figure 3. IR spectrum of calcined pure silica ITQ-4.

The chemical compositions of several ITQ-4 samples synthesized from reaction mixtures containing SDA **I** or **II** at different final pH are listed in Table 2. For the sample synthesized using **I** the C/N ratio is close to the value of the organic additive (14), suggesting the structure-directing agent is occluded intact inside the zeolitic pores. However, there is a small though noticeable decrease in this ratio as the synthesis pH increases (Table 2), which probably reflects an increased decomposition rate of SDA **I** as the pH increases. For the samples synthesized using SDA **II** at low pH a C/N ratio lower than expected (6.5) suggests a decreased thermal stability of this organic additive under the reported synthesis conditions. Thus, the detailed characterization of ITQ-4 has been carried out on samples synthesized using SDA **I**. The integrity of **I** inside the as-made pure silica ITQ-4 is further confirmed by ^{13}C CPMAS NMR spectroscopy, as seen in Figure 4. The chemical analysis indicates that after the synthesis around two molecules of **I** are occluded per unit cell of 32 SiO_2 tetrahedra. In the pure silica material synthesized at a pH $\leq$ 10 (see Table 2 and discussion below) the positive charge of the organic cation is balanced by the equivalent amount of F^- anions, and the ideal chemical composition is $[C_{14}NH_{20}F]_2[Si_{32}O_{64}]$. However, when the final pH of the synthesis is higher, we observe a decrease in the fluorine concentration in the as-made material, as shown in Table 2 and as discussed below.

The interesting result that pure silica ITQ-4 can be synthesized over a relatively wide range of pH conditions by using F^- as a mineralizer offers the opportunity to investigate to some extent the relationship between the fluoride synthesis route (normally carried out at near to neutral pH) and the presence of defects in (high) silica zeolites. The ^{29}Si MAS NMR spectra of four pure silica ITQ-4 samples synthesized at different pH (8.1, 10, 10.4, and 11.2) are shown in Figure 5. It is apparent that while the samples synthesized at relatively high pH show the presence of a relatively small concentration of defects (characterized by the broad band near -100 ppm), the samples synthesized at lower pH show no defects detectable by Bloch decay ^{29}Si MAS NMR. What is most striking from this result is that, under the synthesis conditions reported here, the pH limit for the appearance of defects seems to be very well-defined, lying between 10.0 and 10.4. Moreover, the relationship between the pH and the concentration of Si$-$O$-$Si connectivity defects indeed displays a very sharp boundary, suggesting there is a threshold pH for the appearance of defects, and a further increase in alkalinity does not result in an increased concentration of defects.

A plausible explanation for the observed effect can be proposed assuming a liquid-phase-mediated mechanism for the crystallization of ITQ-4 in which the ionization state of the condensing species must be pH-dependent. If the formation of the crystals requires the condensation of soluble silicate species

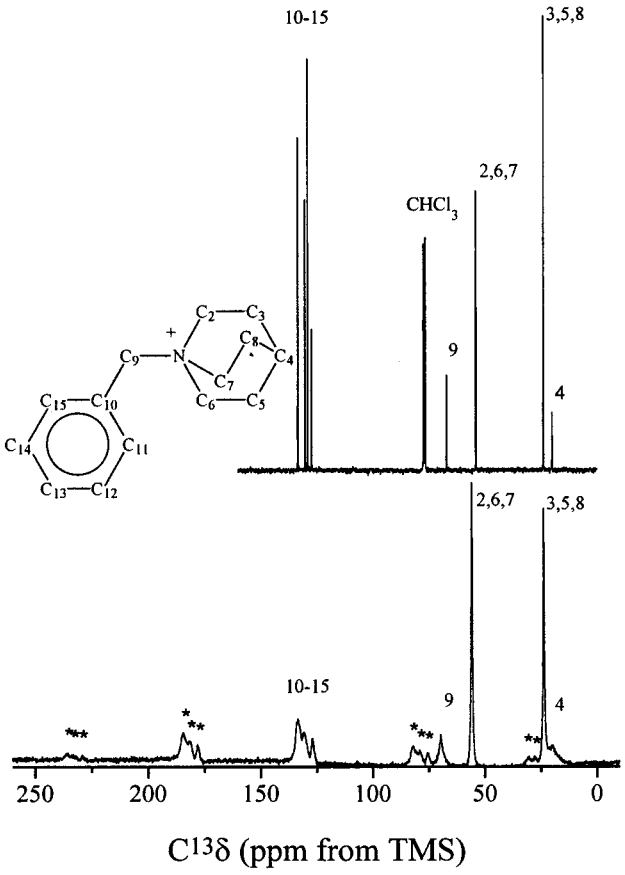

Figure 4. $^1H\rightarrow^{13}C$ CPMAS NMR spectrum of as-prepared ITQ-4 (bottom) and ^{13}C NMR of a $CDCl_3$ solution of the chloride form of SDA **I** (top), showing the assignment of each resonance. Spinning sidebands are marked with a *.

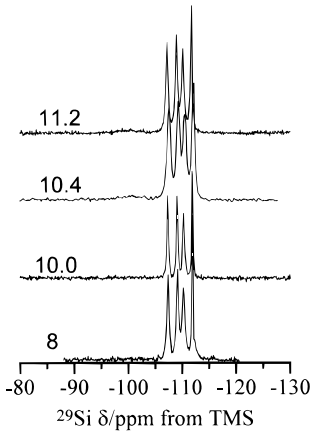

Figure 5. ^{29}Si MAS NMR of calcined pure silica ITQ-4 samples. The numbers near each trace indicate the final pH of the mother liquor.

through a dehydroxylation reaction, then the presence of defects will be governed by two conditions: first, charge balance of the SDA positive charge (which in the presence of entrapped F^- does not require the presence of defects, as well illustrated by ITQ-4 synthesized at pH $\leq$ 10, where the concentration of F^- entrapped in the zeolite closely matches that of the occluded organic cations, see Table 2); and second, the ionization state of the units to be condensed. At pH higher than the pK_a of the condensing species, the concentration of Si$-$O$^-$ terminations will be large and condensation through dehydroxylation will require the protonation of at least one Si$-$O$^-$ group (see Scheme 1, which we note is based purely on stoichiometric considerations, and hence there is no speculation on the precise nature

SCHEME 1

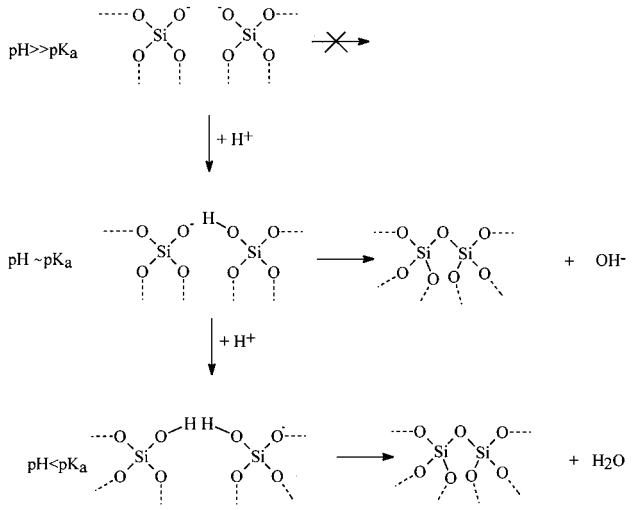

of the condensing species). Thus, under these conditions where Si−O$^-$ species are predominant the formation of defects of connectivity will be favored. On the contrary, at pH lower than the pK_a of the condensing species Si−OH groups will predominate, allowing the condensation of these units to occur very readily, and as a result defect formation will be unfavored (Scheme 1). The observation that there is an abrupt change in the concentration of defect groups in ITQ-4 when going from pH = 10 to 10.4 suggests that the pK_a of the condensing species lies between these limiting values. There is a lack of knowledge concerning the precise nature of the silicate species in solution from which zeolite crystals grow, and furthermore we could actually expect them to change as the pH increases. Even the pK_a can be expected to change as the condensation of other Si−OH groups within the same silicate species proceeds. Thus, we cannot check whether the observation agrees with the pK_a of the condensing species. However, a pK_a value of around 10 for silanol groups looks reasonable. For comparison, the first pK_a of monosilicic acid at 25 °C is about 9.8−9.9 (about 11.7 for the second to fourth pK_a), while the pK_a on the surface of amorphous silica, which is highly dependent on the extent to which the surface is ionized, varies between 6.8 and 9.5, also at 25 °C.[17]

It is interesting to point out that the purely stoichiometric considerations shown in Scheme 1 provide a likely explanation for yet another observed difference between the OH$^-$ (high pH) and the F$^-$ (low pH) synthetic routes. Typically, during the synthesis of zeolites in alkaline conditions there is a significant increase of the pH as the crystallization proceeds.[18] This is a general observation[19] that can be sometimes hidden by the decomposition of the SDA organic cations by a Hoffman degradation or by a buffering effect when the SDA used is an amine. By contrast, the synthesis of pure silica zeolites by the F$^-$ route at near to neutral pH proceeds without significant variations in the pH of the mother liquor. Thus, the crystallization-promoted increase in the OH$^-$ concentration during the synthesis at high pH and the lack of such effect in the F$^-$ method is possibly related to the differences in the ionization state of the condensing species, as reflected in Scheme 1. In the synthesis at high pH the presence of unconnected and deprotonated species (either in solution or in an amorphous phase) allows a lower starting pH, which increases as the crystallization proceeds because of the increasing degree of silica condensation. By contrast, in the synthesis at low pH the increased connectivity

SCHEME 2

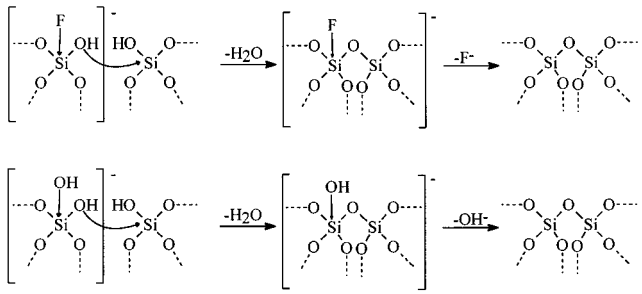

occurs by condensation of protonated species and thus does not lead to a change in pH (Scheme 1).

In this model proposed to explain the observed effects we have not considered in detail the role of F$^-$ and OH$^-$ as mineralizers nor the details pertaining to the mechanism of the condensation at a molecular level. Both anions are thought to be catalysts for the breaking and formation of Si−O−Si bridges. In the case of OH$^-$ it has been proposed that a 5- or 6-fold-coordinated Si is involved in the condensation mechanism[17] and F$^-$ can be speculated to behave in much the same way, given its readiness to form Si−F bonds to give species with larger than 4-fold coordination. Thus, a plausible mechanism for the condensation of silicate species in the crystallization of zeolites can be proposed as follows: the attack of F$^-$ or OH$^-$ upon four-coordinated Si gives a negatively charged pentacoordinated species, which will in turn increase the negative charge of all the O atoms around that Si, favoring the nucleophilic attack on a nearby Si atom (Scheme 2). Under this mechanism, the requirement that at least one of the Si species involved is coordinated to one leaving OH, as shown in Scheme 1, still holds. Thus, the increased concentration of defects as the pH increases beyond a certain critical value is a consequence of the fact that deprotonated species will become predominant at pH > pK_a.

Finally, it should be noted that the chemical analyses of samples synthesized at different pH (Table 2) agree very well with this explanation: for samples synthesized at high pH the concentration of fluorine in the solid is smaller than that of the occluded cation, and thus charge balance requires the presence of a significant proportion of defect sites. By deconvolution of the ^{29}Si MAS NMR spectra we have estimated the relative proportion of Q_3 defect sites as 5−6% in the samples synthesized at high pH, which means there are 1.8−1.9 Si−OH sites in the calcined material. To achieve charge balance, in the as-made solids these defects must be in the form of couples Si−O−H−O−Si (thus, within experimental error in a unit cell the positive charges of 2.1 occluded cations are balanced by the negative charges of nearly 1.2 F$^-$ anions and 0.9 Si−O$^-$ groups). As shown in Table 2, the decrease in F$^-$ concentration parallels the increase in connectivity defects, as there appears to be quite an abrupt change around pH = 10, and beyond this a decreased but constant F$^-$ content in the solids is observed. It is noteworthy that we always found more than one F$^-$ ion per unit cell, while the defect concentration never exceeds one Si−O$^-$ HO−Si couple per unit cell. This could arguably suggest that the stability of the pure silica phase requires either a concentration of F$^-$ higher than 1/uc or a concentration of defects lower than 2/uc, which in turns explains why it appears to be impossible to synthesize the pure silica phase by the OH$^-$ synthesis route.

It is noteworthy that, after calcination to remove the organics, the microporous void volume of ITQ-4 (0.217 cm^3/g measured

by N_2 adsorption experiments)[12] and SSZ-42[20] is surprisingly large for a unidimensional 12MR material, which makes ITQ-4 an attractive material for catalysis (after introduction of Al in the framework)[15] and adsorption applications. We attributed this effect to the high density of pores (separated from each other by a single T-atom wall) together with their sinusoidal nature,[8] while Chen et al. attributed the same effect in a very recent report concerning the structure of the isomorphous alumino(boro)silicate SSZ-42[20] to the presence of so-called cages (which are actually a modulation of the pore size caused by the sinuosity of the channel).

Interestingly, a comparison of the pure silica polymorphs with the lowest framework densities (Table 3, which only includes defect-free materials to avoid a plausible effect of the presence of connectivity defects on the void volume accessible to N_2) shows that there is no correlation between the framework density and the measured void volume. Thus, apparently a fraction of the space not occupied by $SiO_{4/2}$ tetrahedra is nonaccessible to N_2, and we suggest that the presence of small cages could be at least in part responsible for the observed effect, as a different population of cages of different sizes are present in each pure silica structure listed in Table 3.

Analysis of Synchrotron PXRD Data of As-Made Pure Silica ITQ-4. The sample synthesized at a pH = 10.4 was chosen for the structural PXRD study in order to minimize preferred orientation effects (see Figure 2). The recorded synchrotron powder diffraction data sets were normalized and summed before the positions of the first 30 reflections were measured accurately and used to refine the unit cell dimensions obtained from laboratory X-ray diffraction data in the program REFCEL.[21] The new unit cell obtained and the positions of the framework atoms from the calcined structure were taken as the starting model for Rietveld profile refinement[22] using the GSAS suite of programs.[23] A pseudo Voigt function[24] was used to describe the peak shape together with a manually interpolated background. After refinement of the scale factor, unit cell, zero point, and profile parameters the model converged to R_{wp} = 52.7 and R_p = 37.2.

Fourier maps were subsequently employed at this stage to locate the template and template-charge compensating fluorine counterions without success. Both observed and difference Fourier maps calculated at this point did not unambiguously reveal the positions of the fluorine and template atoms missing from the model. Attempts to solve the structure by direct methods using Le Bail extracted intensities (Mprofil5 code)[25] in the program Sirpow[26] succeeded in reproducing the framework structure and the position for the fluorine counterion but found only fragments of organic material having a mixture of expected C−C distances and angles as well as a number of unrealistic ones. Given the complex shape of the *N*-benzyl-1-azoniumbicyclo[2,2,2]octane employed in the chemical synthesis, both rotational disorder of the quinuclidine and benzyl moieties and "channel up" and "channel down" configurations (meaning both possible orientations inside the channels) are conceivable. However, because of the size and shape of the template molecule and the dimensions of the channel, rotation of the whole molecule is prevented.

Using the fragments of organic material obtained from direct methods as a starting point, a model-building approach was adopted in order to try to understand the templating behavior in this material. Various models were constructed within the *I*2/*m* symmetry of differing complexities, of which the final model presented here represents the best model with the required template geometry.

SCHEME 3

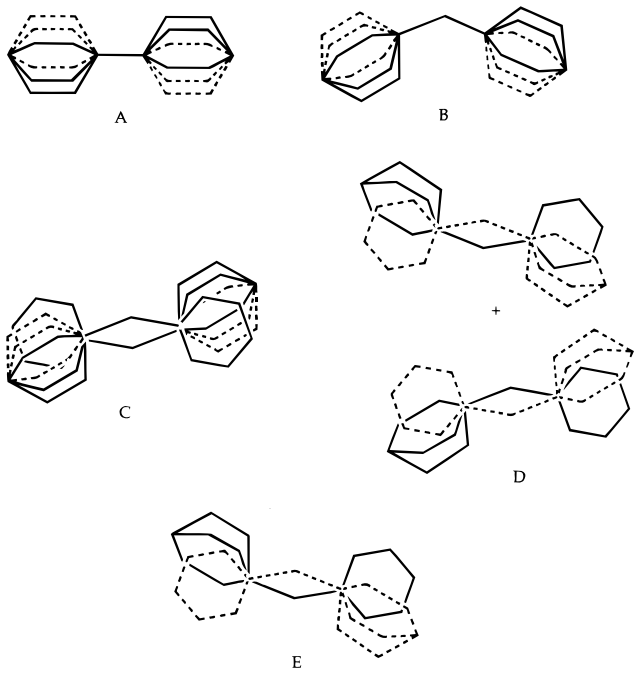

Within the scope of the different models considered both examples of up and down channel template disorder were considered together with those that allowed for some rotation of the constituent rings. Simple models such as A and B (Scheme 3) considering the template as a simple cylindrical shape, while accounting for much of the electron density (for A R_{wp} = 12.67, R_p = 9.46, R_b = 13.71 and R_{wp} = 12.81, R_p = 9.52, R_b = 13.88 for B; see ref 23 for definitions of these residuals), lead to a poor framework geometry. Adopting models of type C in Scheme 3 whereby attempts were made to include benzene positions only marginally improved the residuals (R_{wp} = 12.36, R_p = 9.25, R_b = 13.08) and moreover resulted in a much more unrealistic spread of values for the thermal parameters. Models of type D involve the splitting of the "up" and "down" quinuclidines which formed the cylindrical shape into "left" and "right" configurations when viewed along the *c* crystallographic direction. In essence this model represents the construction of two independent template molecules (and their symmetry equivalents, all template atoms with an occupancy of 0.25) and the symmetry equivalents within the channel structure. While this model resulted in an improvement in the residuals (R_{wp} = 11.92, R_p = 9.08, R_b = 12.93), once again it was found that the temperature factors were very unstable. Furthermore, refinement of the occupancy for the two distinct molecules constraining the total value to be that expected from chemical analysis showed structure E to be much more favorable (occupancy 0.43 per site as opposed to 0.07). Complete removal of the other configuration and full refinement of the model (E) resulted in the lowest residuals (R_{wp} = 11.16, R_p = 8.73, R_b = 12.72) for this model and most realistic thermal parameters. The final model in fact represents a simpler solution whereby the organic molecule can have either channel up or channel down configurations, and thereby rotation in the $a-b$ plane and extensive overlap of the benzene and quinuclidine rings are found to be less satisfactory models for the disorder in this case. In the final stages of refinement the occupancy of the fluorine was also allowed to vary, leading to a further improvement in the residuals (R_{wp} = 10.44, R_p = 7.99, R_b = 10.06) as well as the overall framework bond lengths and angles. We note that the refined occupancy obtained for the fluorine position is in

TABLE 5: Fractional Coordinates, Occupancy, and Isotropic Temperature Factors for As-Prepared ITQ-4 with ESDs in Parentheses

atom	*x*	*y*	*z*	occupancy	$U_{iso} \times 100$
Si(1)	−0.01078(21)	0.10989(28)	0.2935(5)	1.0	1.84(6)
Si(2)	0.24638(23)	0.11497(27)	0.6100(6)	1.0	1.84(6)
Si(3)	0.14845(21)	0.11712(28)	0.2358(7)	1.0	1.84(6)
Si(4)	0.15705(21)	0.20233(28)	−0.1134(6)	1.0	1.84(6)
O(5)	0.3247(4)	0.1800(5)	0.6470(9)	1.0	1.67(10)
O(6)	−0.0689(4)	0.1896(4)	0.2023(10)	1.0	1.67(10)
O(7)	0.00000	0.1225(7)	0.50000	1.0	1.67(10)
O(8)	0.0609(4)	0.1425(4)	0.2372(9)	1.0	1.67(10)
O(9)	0.1540(4)	0.00000	0.2045(14)	1.0	1.67(10)
O(10)	0.1950(4)	0.1429(4)	0.4151(13)	1.0	1.67(10)
O(11)	−0.0340(5)	0.00000	0.2304(14)	1.0	1.67(10)
O(12)	0.2083(4)	0.1337(5)	0.7814(11)	1.0	1.67(10)
O(13)	0.2770(11)	0.00000	0.6146(14)	1.0	1.67(10)
O(14)	0.1792(4)	0.1733(5)	0.0857(12)	1.0	1.67(10)
C(1)	0.82019(19)	0.50000	−0.3666(24)	0.5	9.8(8)
C(2)	0.85606(26)	0.41631(6)	−0.3363(16)	0.5	9.8(8)
C(3)	0.9224(4)	0.41631(6)	−0.2388(18)	0.5	9.8(8)
C(4)	0.95189(19)	0.50000	−0.1759(16)	0.5	9.8(8)
C(5)	0.97269(19)	0.50000	0.0599(19)	0.5	9.8(8)
N(6)	0.95705(28)	0.50000	−0.1386(15)	0.5	13.7(7)
C(7)	0.9901(4)	0.40881(4)	−0.2036(21)	0.5	13.7(7)
C(8)	0.9746(7)	0.40881(4)	−0.4022(21)	0.5	13.7(7)
C(9)	0.9311(7)	0.50000	−0.4697(19)	0.5	13.7(7)
C(10)	0.87519(31)	0.50000	−0.2073(17)	0.5	13.7(7)
C(11)	0.8596(6)	0.50000	−0.4059(18)	0.5	13.7(7)
F(1)	0.8410(13)	0.00000	0.430(4)	0.311(15)	4.3(22)

very good agreement with the results from chemical analysis (refined, 1.24 F^-/uc; found by chemical analysis, 1.13 F^-/uc; see Table 2).

In the final model and for all the models attempted soft constraints were applied to the C−C (N) and C−C−C (N) bond lengths and angles, respectively, with in addition the occupancies for the organic template atoms fixed to be that expected from chemical analysis. Also, as for the structure analysis of the calcined sample,[8] a preferred orientation correction was necessary because of the elongated shape of the crystallites. In the final cycles of refinement all the atomic positions and temperature factors were fully refined, with the final model converging to the residuals given in Table 4. The final atomic coordinates and isotropic temperature factors are presented in Table 5 with the final Rietveld plot given in Figure 6.

Structure of As-Made ITQ-4[$(C_{14}H_{20}NF)_{2.1}(Si_{32}O_{64})$]. ITQ-4 (IFR) is a one-dimensional zeolite characterized uniquely by virtue of its sinusoidal 12-ring channel parallel to the *c* crystallographic direction in space group *I*2/*m*. Also of technological interest in this material is its large micropore volume (Table 3), which we can understand as a consequence of the high density of channels provided by the small (single four-membered ring) separation between them. Around the perimeter of the channels there are small [$4^3 5^2 6$] cages within which the fluorine counteranions are found to be located (Figure 7). This observation is in good agreement with other structures in which fluorine has been located, showing the preference of these ions for small secondary cagelike units.[27−29] In that sense, in addition to its mineralizing role during the synthesis of crystalline microporous materials, F^- is sometimes claimed to be a structure-directing agent and even a template.[5] However, one should expect a low geometric specificity for the interactions between F^- and the framework cages, if one imagines F as an approximately spherical ion. In fact, F^- has been found in several different types of cages, showing different sizes and geometries, and thus the concept of F^- as a template is at least dubious, if the proper and restricted definition of template proposed by Davis and Lobo (based on a close geometric correspondence between the template entity and the zeolite framework) is assumed.[30]

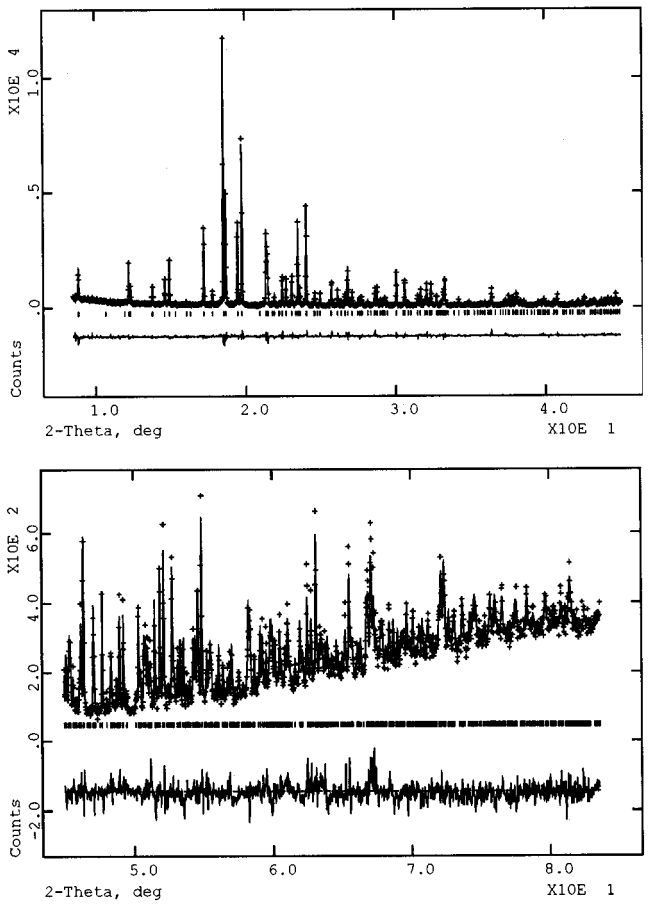

Figure 6. Observed (+) and calculated (solid line) X-ray diffraction patterns for pure silica as-prepared ITQ-4 (wavelength 1.39996 Å) following Rietveld refinement. Vertical ticks indicate the positions of allowed reflections in space group *I*2/*m*. The lower trace is the difference plot.

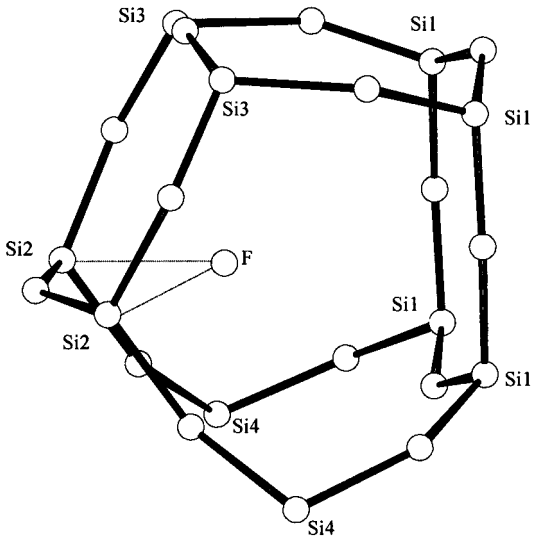

Figure 7. Structure of the [$4^3 5^2 6$] cage in as-prepared ITQ-4 showing the location of the fluorine counterion and the closest F−Si distances of 2.2 Å (dotted lines).

The location of F^- in the [$4^3 5^2 6$] cages of ITQ-4 is rather similar to its location in the MFI and cobalticinium-NON structures. In all of these phases F^- is located in front of a 4MR unit inside a small cage. In the case of the NON framework single crystal structure analysis unambiguously

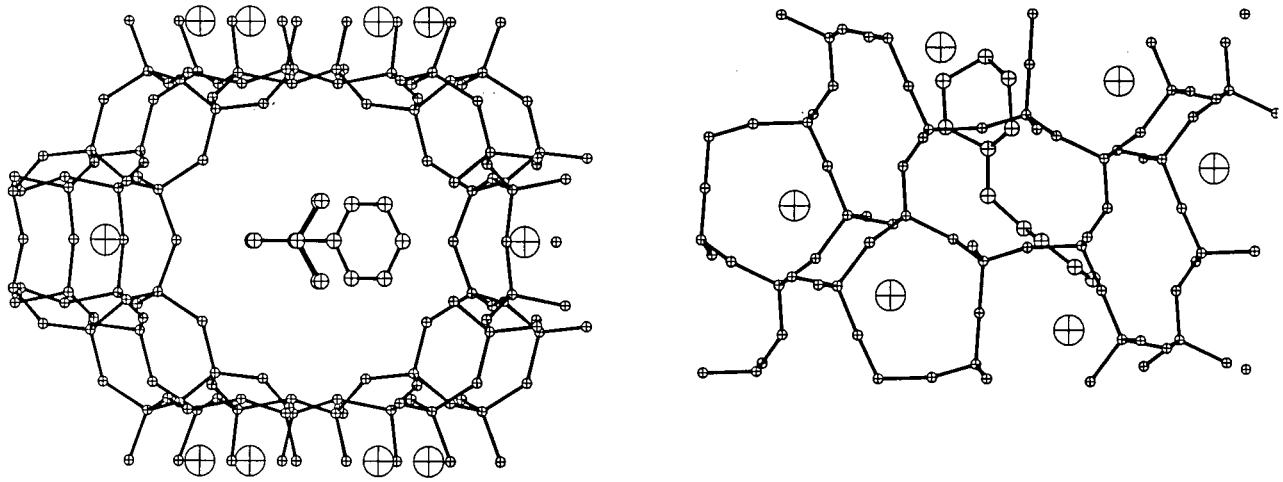

Figure 8. Structure of as-prepared ITQ-4 showing for clarity the location of only one of the template cations. Left: projected along the 12MR (*c* crystallographic axis). Right: projection along the floor of the channel (*b* crystallographic axis). Big circles are F^- ions, medium circles are C and N atoms of the SDA **I**, and small circles are Si and O atoms in the framework.

demonstrates the 5-fold coordination of Si atoms involved in Si−F bonds, with a nearly ideal trigonal-bipyramidal geometry.[27] Such bonds have been considered responsible for resonances near −145 ppm in the ^{29}Si and ^{19}F−^{29}Si MAS NMR spectra of cobalticinium-NON.[31] In the case of MFI, X-ray diffraction analyses did not show the presence of Si−F bonds, with the minimum Si−F distances being rather large (2.20 Å)[32] compared to those in NON (1.836 Å). However, ^{1}H−^{29}Si and ^{19}F−^{29}Si MAS NMR spectra suggested the existence of such bonds and a dynamic situation at room-temperature involving F^- exchange between different Si atoms.[31] The fast exchange could explain the large Si−F distance found by X-ray analysis. In the case of ITQ-4, the F−Si distances are much like those determined by XRD in MFI. However, so far we found no NMR evidence for such bonds in ITQ-4 (see above), and thus, at present no pentacoordinated Si can be claimed in this structure.

The template itself is found to be located diagonally across the [$4^2$6^4] cage in the floor of the channel when viewed in the *ac* plane of the structure (Figure 8). The *I*2/*m* symmetry of the structure leads to a quinuclidine bridge up and bridge down alternation along the channel modulation by 2-fold rotation. This symmetry operation produces an unrealistically close separation (1.93 Å) between the bridge up and bridge down quinuclidine units at each cavity connection (Figure 9), if we consider the channel as the stacking of cavities within which the template resides. This suggests that within a given channel there is template order or the presence of one defect (benzene...benzene) which will immediately revert back to an ordered configuration within any one channel. However this analysis suggests firmly that in a different channel the converse is likely to apply (i.e., the templates aligning in the opposite configuration), providing an explanation for the complex nature of the calculated Fourier maps and the results obtained by direct methods. In essence, there is order or a unique defect within a single channel but template disorder over the complete structure when viewed as a whole. The benzene ring is found to be located across the mirror plane beneath the 4-ring facing inward to the channel of the [$4^3$5^{2}6] cage unit. The isotropic temperature factor for this occluded species while comparing in magnitude to other templated structures indicates there to be some movement and rotation of the template about this idealized position. However for the other models tried the temperature factors were consistently observed to take on unrealistic values, indicating

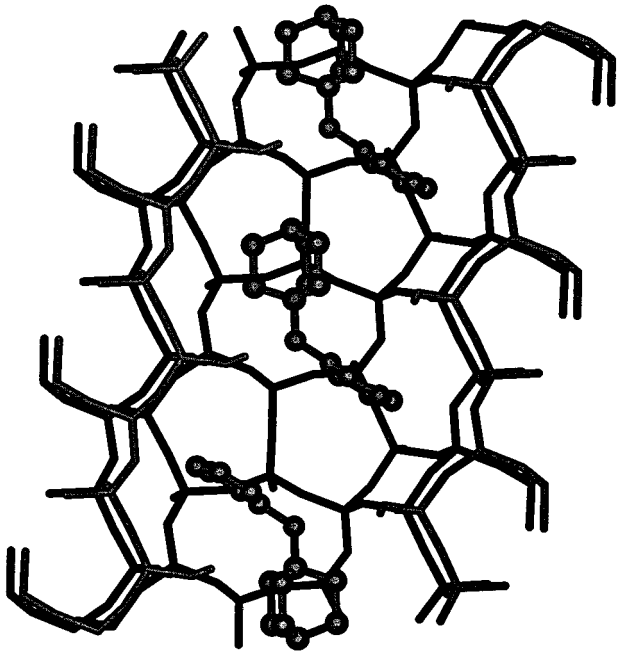

Figure 9. Template orientations in ITQ-4, showing three template molecules in the two possible conformations, "bridge up" and "bridge down". We note that within a single channel only one defect is allowed to exist (benzene...benzene, as shown by the lower two template molecules), which effectively reverses the template orientation. To summarize, we could expect within a single channel a sequence of conformations that is completely ordered (quinuclidine−benzene−quinuclidine...), its inverse (benzene−quinuclidine−benzene...), or the presence of a single defect (quinuclidine−benzene...benzene−quinuclidine).

that these other models did not represent a correct distribution of electron density.

In more general terms and with particular regard to the premise of structure direction, the template is not found to follow the complete curvature of the channel but remains localized with one diagonal of the overall "zigzag" pattern of the pore structure. From the arguments presented earlier suggesting that within a single channel there is a high degree of template order, there appears to be a reasonable agreement between the bent shape of the template and the pore architecture. This applies equally to the "up" and "down" channel configurations, providing support for this molecule as a structure-directing agent showing a limited but noticeable geometric correspondence with the void

volume it occupies, and thus shedding some light on the origin of the unique channel geometry present in ITQ-4.

Acknowledgment. The authors greatly acknowledge financial support by the Spanish CICYT (project MAT97-0723). We thank the CLRC for provision of the synchrotron radiation facilities. P.A.B. is grateful to the European Union TMR program for a postdoctoral fellowship. M.A.C. thanks Dr. H. Koller for providing a copy of ref 31 before publication.

Supporting Information Available: Selected framework atom bond distances and angles and nonframework atom distances and angles for as prepared ITQ-4 (2 pages). Ordering information is given on any current masthead page.

References and Notes

(1) Barrer, R. M. *Hydrothermal Chemistry of Zeolites*; Academic Press: London, 1982.

(2) Kessler, H.; Patarin, J.; Schott-Darie, C. In *Advanced Zeolite Science and Applications*; Jansen, J. C., Stöcker, M., Karge, H. G., Weitkamp, J., Eds.; Elsevier: Amsterdam, 1994; p 75.

(3) Koller, H.; Lobo, R. F.; Burkett, S. L.; Davis, M. E. *J. Phys. Chem.* **1995**, *99*, 12588.

(4) Blasco, T.; Camblor, M. A.; Corma, A.; Esteve, P.; Guil, J. M.; Martínez, A.; Perdigón-Melón, J. A.; Valencia, S. *J. Phys. Chem.*, **1998**, *102*, 75.

(5) Guth, J. L.; Kessler, H.; Caullet, P.; Hazm, J.; Merrouche, A.; Patarin, J. In *Proceedings International Zeolite Conference*; von Ballmoos, R., et al., Eds.; Butterworth-Heinemann: London, 1993; p 215.

(6) Camblor, M. A.; Corma, A.; Valencia, S. *Chem. Commun.* **1996**, 2365.

(7) Camblor, M. A.; Corma, A.; Lightfoot, P.; Villaescusa, L. A.; Wright, P. A. *Angew. Chem., Int. Ed. Engl.* **1997**, *36*, 2659.

(8) Barrett, P. A.; Camblor, M. A.; Corma, A.; Jones, R. H.; Villaescusa, L. A. *Chem. Mater.* **1997**, *9*, 1713.

(9) Guth, J. L.; Wey, R. *Bull. Soc. Fr. Minéral. Cristallogr.* **1969**, *92*, 105.

(10) Cernik, R. J.; Murray, P. K.; Pattison, P.; Fitch, A. N. *J. Appl. Crystallogr.* **1990**, *23*, 292.

(11) Villaescusa, L. A.; Camblor, M. A.; Corma, A. Spanish Pat. 9602685, 1996.

(12) Camblor, M. A.; Corma, A.; Villaescusa, L. A. *Chem. Commun.* **1997**, 749.

(13) Zones, S. I.; Rainis, A. PCT/US95/01412, 1995.

(14) Valyocsik, E. W. U.S. Pat. 5437855, 1995.

(15) Barrett, P. A.; Camblor, M. A.; Corma, A.; Villaescusa, L. A. Manuscript in preparation.

(16) Flanigen, E. M.; Patton, R. L. U.S. Pat. 4073865, 1978.

(17) Iler, R. K. *The Chemistry of Silica*; John Wiley and Sons: New York, 1979.

(18) Lowe, B. M. *Zeolites* **1983**, *3*, 300.

(19) (a) Casci, J. L.; Shannon, M. D.; Cox, P. A.; Andrews, S. J. In *Molecular Sieves*; Occelli, M. L., Robson, H., Eds.; Van Nostrand Reinhold: New York, 1992; p 359. (b) Camblor, M. A.; Pérez-Pariente, J. *Zeolites* **1991**, *11*, 202.

(20) Chen, C. Y.; Finger, L. W.; Medrud, R. C.; Crozier, P. A.; Chan, I. Y.; Harris, T. V.; Zones, S. I. *Chem. Commun.* **1997**, 1775.

(21) Refcel Program for unit cell refinement, Daresbury Laboratory.

(22) Rietveld, H. M. *J. Appl. Crystallogr.* **1969**, *2*, 65.

(23) Larson, A.; Von Dreele, R. B. GSAS Manual, los Alamos Report No. LA-UR-86-748, 1986.

(24) Hastings, J. B.; Thomlinson, W.; Cox, D. E. *J. Appl. Crystallogr.* **1984**, *17*, 85.

(25) Le Bail, A. *Mater. Res. Bull.* **1988**, *23*, 447.

(26) Murray, A. D.; Fitch, A. N. Mprofil Program for Le Bail Decomposition and Profile Refinement, 1990.

(27) van de Goor, G.; Freyhardt, C. C.; Behrens, P. *Z. Anorg. Allg. Chem.* **1995**, *621*, 311.

(28) Simmen, A.; Patarin, J.; Baerlocher, Ch. In *Proccedings of the 9th International Zeolite Conference*; von Ballmoos, R., et al., Eds.; Butterworth-Heinemann: London, 1993; p 433.

(29) Camblor, M. A.; Díaz-Cabañas, M. J.; Pérez-Pariente, J.; Teat, S. J.; Clegg, W.; Shannon, I. J.; Lightfoot, P.; Wright, P. A.; Morris, R. E. *Angew. Chem., Int. Ed. Engl.*, in press.

(30) Davis, M. E.; Lobo, R. F. *Chem. Mater.* **1992**, *4*, 756.

(31) Koller, H.; Wölker, A.; Eckert, H.; Panz, Ch.; Behrens, P. *Angew. Chem., Int. Ed. Eng.* **1997**, *36*, 2823.

(32) Mentzen, B. F.; Sacerdote-Peronnet, M.; Guth, J. L.; Kessler, H. *C. R. Acad. Sci. Paris* **1991**, *313*, 177.

(33) Camblor, M. A.; Corma, A.; Diaz-Cabañas, M. J.; Baerlocher, Ch. *J. Phys. Chem.* **1998**, *102*, 44.

(34) Camblor, M. A.; Corell, C.; Corma, A.; Díaz-Cabañas, M. J.; Nicolopoulos, S.; González-Calbet, J. M.; Vallet-Regí, M. *Chem. Mater.* **1996**, *8*, 2415−2417.